Chapter 8

# Architecture of the Gas Exchange Region of the Lungs

Robert R. Mercer and James D. Crapo

## Chapter Outline



## 1. INTRODUCTION

The architectural arrangement of the small airways and distal gas-exchange region in the lungs is obviously critical in determining the sites of deposition of gases and particles, as well as in subsequent tissue responses due to injury. In this chapter, we will cover the results of quantitative determination of the structure of the small airways and gas-exchange regions of the lungs. Because extrapolation of experimental studies in laboratory animals to the adverse health effect in humans is a central interest, we will be particularly interested in comparing the structure of the gas-exchange region of different species and the implications that these differences in structure have on dosimetry. The complex architecture of the pulmonary airway system has made the calculation of dose of inhaled pollutants delivered to specific sites in different species a difficult process. This difficulty is particularly apparent in the lack of structural data describing the gas-exchange regions of the lungs where low level, chronic exposures to reactive gases and aerosols have their most significant effects. The focus on injury in the gas-exchange region has been demonstrated for inhaled oxidant gases (Crapo et al., 1984), asbestos (Pinkerton et al., 1986), silica (Scabilloni et al., 2005), and newly developed nanomaterials such as titanium dioxide (McKinney et al., 2012) and carbon nanotubes (Porter et al., 2012; Mercer et al., 2013).

Detailed and quantitative assessments of the structure of the gas-exchange region in the lungs is a relatively recent task undertaken by a number of laboratories. For example, Weibel's (1963) model of the respiring region of the human lung was not a direct measurement and was based on the assumptions that the airways branch dichotomously up to the bronchiole-alveolar duct junction, with three generations of alveolar ducts proceeding out to the alveolar sac. The model of Yeh et al. (1979), based on the study of a single corrosion cast of a rat lung, also included an extrapolation of the acinar region of the rat using Weibel's model of the human lung scaled down to the alveolar dimensions in the rat lung. The advent of new stereological methods for estimating size and number, the development of quantitative methods for analyzing structure using serial section reconstructions, and the analysis of casts made of the gas-exchange region in the lungs have provided a more rigorous and detailed knowledge of the structural arrangement of the gas-exchange region in the lungs. Data from these techniques are being used to determine the extent to which differences in acinar structure between different species influence pulmonary dosimetry in laboratory animals and humans, and the significance that variations in acinar size, branching pattern, and other structural features may have on the homogeneity of lesions following inhalation of airborne pollutants.

## 2. DEFINITIONS

There is a wide range of terms used in describing the terminal airways and gas-exchange region of the lungs.

Comparative Biology of the Normal Lung. http://dx.doi.org/10.1016/B978-0-12-404577-4.00008-4

The pulmonary acinus is perhaps the most commonly used definition, which we can use as a basis for quantitation of lung structure. The word acinus, Latin for grape-like, is a general term used in anatomical nomenclature to indicate a sac-like structure. In the case of the lungs, this nomenclature arises quite naturally from examination of casts of the lung where one finds an airway branch that connects a distal unit containing the gas-exchange surfaces of the lung in the form of respiratory bronchioles, alveoli, and alveolar ducts. Although this definition is relatively simple in concept, there is considerable difficulty in applying it to quantitative studies of lung structure in different species.

The difficulty is particularly apparent when one examines smaller laboratory animals that either lack or have only rudimentary respiratory bronchioles. In these cases, Yeh et al. (1979) have defined the acinus to include the alveoli and alveolar ducts distal to the final airway epithelial termination, with the terminal bronchiole being the airway proximal to the epithelial termination. Rodriguez et al. (1987) have taken it to be the largest parenchymal lung unit where all airways are alveolated. When applying the definitions used by Yeh et al. (1979) or Rodriguez et al. (1987), there is considerable difficulty in comparing gas-exchange structures across different species. Mice do not have respiratory bronchioles. Respiratory bronchioles in the rat are limited to very short segments with only occasional alveolar outpockets, while larger species, such as the human, have one or more generations of respiratory bronchioles (Figure 1). Applying the definition of Yeh et al. (1979) or that of Rodriguez et al. (1987), it is a common occurrence to make the decision concerning the size of the collection of alveoli and alveolar ducts that constitutes an acinus based on the presence or absence of one alveolar outpocket in the short, final airway segment of the rat.

Fortunately there is a definition, corresponding to a collection of alveoli and alveolar ducts, which has a sac-like outer boundary, can easily be identified and counted, and eliminates difficulties in comparison of species with widely differing branching patterns in their small airways and absent or extensive respiratory bronchioles. Storey and Staub (1962) proposed a basic unit of ventilation or, as we will refer to it, a ventilatory unit, which consists of the alveoli and alveolar ducts distal to the transition from one bronchiole to an alveolar duct system. Based on serial section reconstructions, we have demonstrated (Mercer and Crapo, 1987b) that the alveoli and alveolar ducts of ventilatory units occur in a highly interconnected pattern and do not protrude into adjacent units. Thus, this definition leads to subdivisions of the lung consisting of a highly interconnected collection of alveoli and alveolar ducts, as shown in Figure 1. This definition may be used to compare species differences in gas-exchange structure because the bronchiole-to-alveolar duct junction is unambiguously present in all species, whether the immediately proximal airway a respiratory or terminal bronchiole.

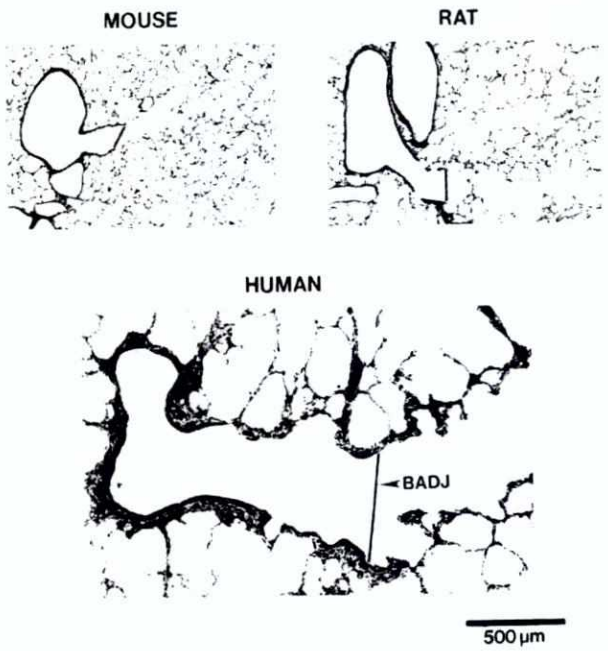


**FIGURE 1 Light micrographs of bronchiole–alveolar duct junctions of mouse, rat, and human lungs.** These micrographs demonstrate the bronchiole–alveolar duct junctions of various species. There is significant variation in the geometry of the airway immediately proximal to the bronchiole–alveolar duct junction. For instance, there are no alveoli in the walls of the very short final airway of the mouse, while the airway in the human lung is 1–2 mm in length and contains numerous alveolar outpockets.

The ventilatory unit is functionally important because it is the smallest common denominator in determining the distribution of inspired gas to the gas-exchange surfaces of the lungs. Thus, the ventilatory unit has a central role when considering what effect variations in size and architecture have in determining the dose of inhaled pollutants delivered to the gas-exchange region.

Figure 2 provides a schematic view of a lung illustrating the various anatomical descriptions that are used in subsequent descriptions. These include the subdivision of the lung that consists of the final terminal bronchiole dividing the distal alveoli-alveolar ducts into two or more units, distal respiratory bronchioles and ventilatory units. We note that this subdivision is also sometimes referred to as an acinus. However, it is clear from serial section analysis of the gas-exchange region of different species, such as illustrated in Figure 2, that more than one sac-like cluster of alveoli and alveolar ducts is distal to a single terminal bronchiole. The gas-exchange structure within each ventilatory unit is composed of alveolar ducts and the encircling alveoli.

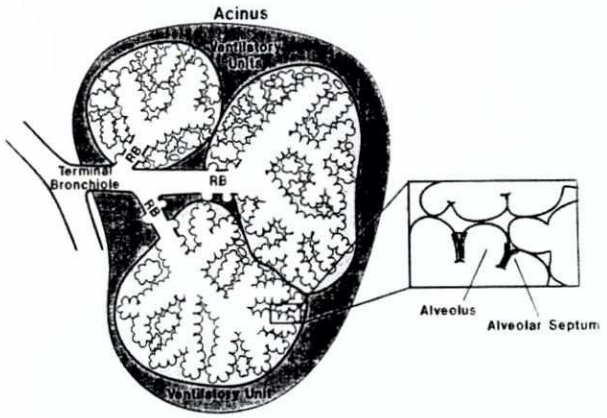


**FIGURE 2 Components of the acinus.** This figure illustrates the components of the acinus. These include the terminal bronchiole dividing the distal alveoli-alveolar ducts into two or more ventilatory units and the respiratory bronchioles (RB). Each ventilatory unit consists of the alveoli and alveolar ducts distal to a single bronchiole–alveolar duct junction. Three ventilator units are illustrated in this example.

## 3. METHODS OF STUDY

The basic methods used to study the gas-exchange region of the lungs consist of: (1) study of the small airways by casting techniques; (2) determination of the number of gas-exchange structures, either acini, ventilatory units, or alveoli, by the use of stereological techniques; and (3) determination of the structural relationships between different components by quantitative measurements of number, size, and diffusional characteristics using serial section analysis techniques. Each of these methods has inherent advantages and limitations. For instance, casting of the lungs is relatively simple to carry out, and the subsequent manual measurements do not require elaborate instruments. However, casting techniques do not preserve the delicate arrangement of the surfactant-lined surfaces of alveoli and alveolar ducts, because the installation of the fluid casting material destroys the critical air-to-tissue barrier and reexpands the lung in a nonhomogeneous manner (Gil et al., 1979). On the other hand, stereological methods for estimating number are efficient and accurate, and can be applied to lungs fixed in any manner (Mercer et al., 1987; Randell et al., 1989). However, the quantitative descriptions provided by stereological techniques are limited to determining the number of units and the average size of the unit, and do not allow the measurement of parameters critical to the characterization of the gas-exchange process, such as alveolar duct diameter or length.

Quantitative serial section analysis technique may also be used to analyze lungs preserved in any of a number of ways. In particular, the most appropriate of these is to use vascular perfusion-fixed lung preserved at levels of lung volume comparable to functional residual capacity. In this way, the structure of the lungs may be preserved in a state most nearly approximating that present during normal breathing. Since serial section analysis techniques are based on entry of the three-dimensional structure of the gas-exchange region of the lungs into a computer, the types of analysis that may be performed are virtually unlimited. Indeed, quantitative serial section analysis techniques have been used to determine ventilatory unit size, number of alveoli per ventilatory unit, alveolar duct branching pattern, and alveolar duct length, and to provide an estimate of the diffusional distance present in the gas-exchange region of different species. The major limitation of this technique is the difficulty and expense of entry of the structure into digital form for numerical and visual analysis. In particular, previous studies have usually included hundreds or even thousands of sections to be entered. Recent studies have shown that the number of sections required to achieve a high accuracy in numerical analysis based on serial sections is significantly smaller than that used in previous studies (Mercer et al., 1990a,b). In addition, advances based on systematic sampling (Gundersen and Jensen, 1987) in a series of sections have been developed that do not require computer entry (Mercer and Crapo, 1989).

## 4. COMPARISONS OF STRUCTURE ACROSS SPECIES

Over the size of mammalian lungs from shrew to whale, the mechanical characteristics of the lungs determined from pressure versus volume behavior and other measures of pulmonary function are remarkably similar (Leith, 1976; Schroter, 1980). As we shall demonstrate, this similarity in mechanical function is paralleled by similarity in the structural determinates of gas exchange.

Table 1 displays the quantitative results describing the acinar structure reported for various species by a number of investigators. Although there are some discrepancies and differences in methodology, the results demonstrate a remarkably smooth transition in number, volume, and dimensions of the acinus as one progresses from mouse to human lungs. Over the range from mouse to human lung, there is an approximately 50-fold increase in acinar number, a 170-fold increase in acinar volume, and a 7-fold increase in acinar diameter.

In spite of these large changes in volume, surface area, and other absolute measures, the pattern or structural arrangement of the gas-exchange unit is remarkably similar. For instance, the average number of generations of alveolar ducts in a single unit is approximately the same across species. This is somewhat unexpected, since different investigators approximate the closely spaced and irregular-shaped branches of the alveolar ducts in different manners. For instance, Parker et al. (1971) stated that essentially all trifurcations could be subdivided into

**TABLE 1 Acinar Morphometry**

| Species | References | TBD (mm) | #/Lung | V ($mm^3$) | D or L (mm) | # Alveoli | Alveolar Duct Generations |
|---|---|---|---|---|---|---|---|
| Human | Pump (1964) | 0.58 | | 1.33–30.9 | | 15,000 | |
| | Horsfield and Cuming (1968), Parker et al. (1971) | 0.60 | 27,992 | | | 10,714 | 6 |
| | Hansen and Ampaga (1975), Hansen et al. (1975) | 0.58 | 23,000 | 160.8 | 7.04 (L) | 14,000–20,000 | 9 |
| | Boyden (1971) | | 80,000 | 15.6 | | | 2–5 |
| | Schreider and Raabe (1981) | 0.43 | | | 5.1 (L) | 7100 | 8–12 |
| | Haefeli-Bleuer and Weibel (1988) | 0.50 | 26,000–32,000 | 187.0 | 8.8 (L) | 10,344 | 9 |
| | Mercer, personal communication | 0.5 | 43,000 | 200.0 | 6.0 (L) | 8000 | 9 |
| Baboon | Mercer and Crapo (1988b) | 0.4 | 32,000 | 15.0 | 2.9 (D) | 5094 | 8–2 |
| Rabbit | Kliment (1973) | | 17,900 | 2.54 | | | |
| | Rodriguez et al. (1987) | | | 3.46 | 1.95 (L) | | 6 |
| Guinea pig | Kliment (1973) | | 5100 | 1.25 | | | |
| | Mercer, personal communication | | 4097 | 1.09 | 1.56 (D) | 6890 | 9–12 |
| Rat | Kliment (1973) | | 2500 | 1.3 | | | |
| | Yeh et al. (1979) | | 2487 | 5.06 | | | |
| | Mercer and Crapo (1987b) | 0.21 | 2020 | 1.9 | 1.5 (D) | 5243 | 10–12 |
| | Rodriguez et al. (1987) | | | 1.46 | 1.46 (D) | | 6 |
| Mouse | Mercer and Crapo (1988b) | | 1025 | 0.3 | 0.9 (D) | 4208 | 8–11 |

TBD, terminal bronchiole diameter; #/Lung, # units per lung; V, unit gas exchange volume; D or L, unit diameter or length.
# Alveoli, # alveoli per unit; Alveolar duct generations, average # of alveolar generations from first alveolar duct to alveolar duct of a terminal sac.

successive bifurcations separated by a very narrow alveolar duct segment. In large part, this technical issue reflects the fact that the convenient, right circular cylinder model is used to approximate the actual structure of the alveolar ducts.

In our studies of alveolar ducts, we have found that the length of the alveolar duct segments between bifurcations was approximately equal to the alveolar duct diameter (Mercer and Crapo, 1987b). It was also found that the distance for each unique path of the alveolar duct network from the bronchiole-alveolar duct junction to the most distal region in the acinus was approximately equal to the ventilatory unit diameter. These results are not consistent with the traditional descriptions of the alveolar duct network as a linear, fanlike network of long, narrow tubes. It is thus more appropriate to consider the matrix of alveoli and alveolar ducts distal to the bronchiole-alveolar duct junctions as a three-dimensional lattice or honeycomb that fills a semispherical space.

In this respect, it is of particular interest to note that the number of alveoli used to fill the space occupied by the acinus is relatively constant between species. We have found in our studies that the ventilatory unit size and alveolar size increase in direct proportion in various species, as indicated in Figure 3 (Mercer and Crapo, 1988a; Mercer et al., 1991, 1994). The results from Figure 3, combined with the relatively constant number of alveoli per acinus, indicate that alveoli and alveolar duct structures in larger species are a scaled-up version of that present in smaller species, with no additional complexity in the arrangement or number of alveolar ducts and alveoli.

Not all aspects of acinar structure are similar across species. Most obvious of these is the difference in the structure and arrangement of the bronchioles supplying the gas-exchange region of different species. In addition to the differences in airways proximal to the bronchiole-alveolar duct junction, one finds significant differences

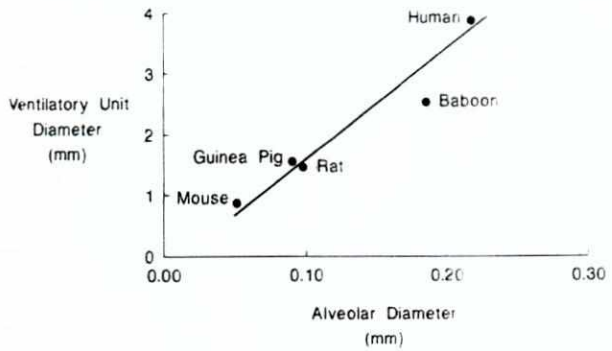


**FIGURE 3 Alveolar versus ventilatory unit diameter.** The alveolar diameter versus ventilatory unit diameter from lungs of different species preserved by vascular perfusion fixation at lung volumes comparable for functional residual capacity. A remarkable similarity in structure is demonstrated by the fact that the ratio of ventilator unit diameter to alveolar diameter is constant over the large range of lung size examined, with the ventilatory unit being 17.5 alveolar diameters in size.

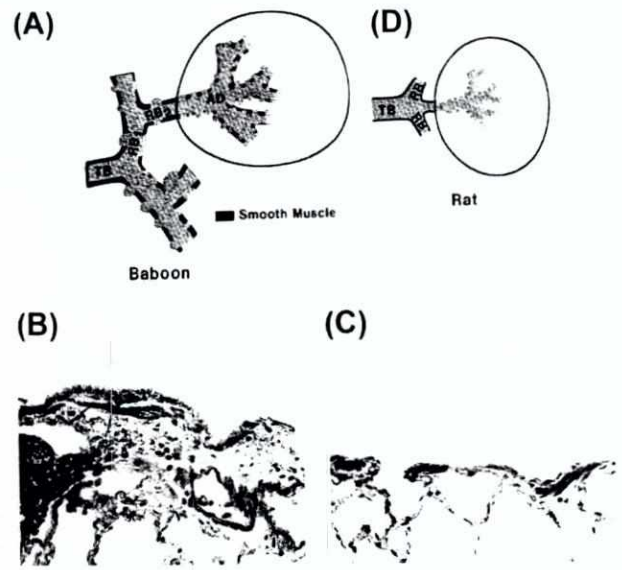


**FIGURE 4 Extent of smooth muscle fibers in the ventilatory unit.** The differences between species in the extension of smooth muscle fibers into the ventilatory unit are illustrated in this figure. In the lungs of humans, baboons, and guinea pigs, the smooth muscle system present in the final airways extends out into the alveolar duct system, as illustrated in (A) and the accompanying light micrographs of a respiratory bronchiole (B) and an alveolar duct from the central acinar region (C). For mice, rats, and other mammals, the smooth muscle fibers terminate at the bronchiole-alveolar duct junction, as illustrated in (D).

with regard to the extension of smooth muscle from the bronchiole–alveolar duct junction out into the alveolar ducts. For guinea pig (Nadel, 1964), baboon, and human lungs (Macklin, 1929), the fibers of smooth muscle derived from the airways extends out into the first few generations of alveolar ducts, as is illustrated in Figure 4. In the lungs of rats and mice, smooth-muscle fibers do not extend past the bronchiole–alveolar duct junction. This network of smooth muscle can profoundly affect gas exchange, as originally demonstrated by Nadel et al. (1964) in the guinea pig.

Because this network of smooth muscle is just beneath the thin alveolar epithelium, it is obviously more susceptible to injury by reactive airborne gases that can penetrate several microns into alveolar tissue (Miller et al., 1982; Overton et al., 1989) than smooth muscle fibers beneath the much thicker airway epithelium. Thus, the smooth muscle fibers in the alveolar region are susceptible to attack by inhaled pollutants and may play a role in the rapid changes in respiratory mechanics following very short exposures to ozone in these larger species (Fouke et al., 1988).

## 5. VARIATION IN SIZE

Analysis of the branching patterns of the airways using casts (Horsfield and Cumming, 1968; Yeh et al., 1979; Ross, 1957) and by serial section analysis (Mercer and Crapo, 1989; Mercer et al., 1991) has demonstrated that there are significant variations in the volume of anatomic dead space from trachea out to the acinus. For instance, Horsfield and Cumming (1968) calculated that a greater than four-fold difference in transit time exists from the canna to distal respiratory bronchioles based on analysis of a single human lung cast. Such variations in airway dead space when applied to problems of either gas exchange or dosimetry of inhaled pollutants can lead to significant regional variation between different lobes (Overton et al., 1989).

A major assumption made in all models of gas exchange or dosimetry based on the analysis of airway dead space variations has been that the ventilation to each acinus and its ventilatory unit subdivisions is constant throughout the lungs (Miller et al., 1982; Overton et al., 1989). Thus, current models of gas exchange and dosimetry of the lungs have been based on a homogeneously ventilating lung, where acinar size and ventilation are constant between different units and regions. However, as early as the studies of Boyden (1971), it has been known that there is a considerable variation in the size of different acini due to different growth rates during development. For instance, Boyden (1971) states that "one leaves this study feeling that so great is the fight for space in the post natal years of growth and differentiation that the end-result is a highly variable and individualist pattern." Boyden made these conclusions based on physical models derived from serial sections of lungs fixed by intratracheal instillation of fixative. Rodriguez et al. (1987) and Haefeli-Bleuer and Weibel (1988), using casting techniques in lungs, preserved near-total lung capacity and concluded that there were variations in size of acini over the entire lung. However, neither of these studies looked at lungs perfused by vascular perfusion fixation and therefore do not describe the distributions of acinar size that would be present at normal levels

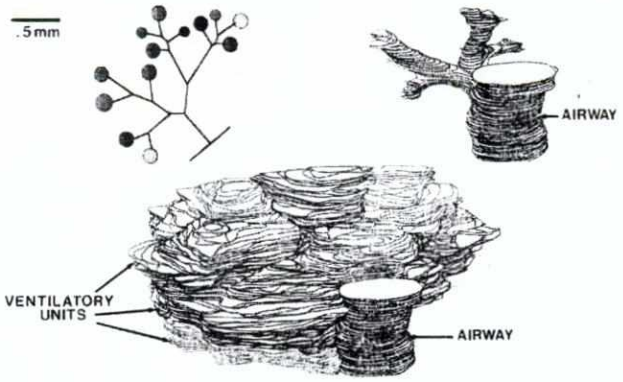


**FIGURE 5 Hidden line view of a three-dimensional reconstruction of the airways and distal ventilatory units from a rat lung.** A stick-like figure of the airway branching pattern with color-coded circles representing the ventilator units is given in the upper left. The diameter of each circle is proportional to the alveolar air volume of each ventilator unit. Three-dimensional reconstructions of the airways distal to the main stem bronchus and the outer boundary of each ventilator unit are given in the upper right and bottom middle of the figure, respectively. This particular example was chosen as it is relatively simple, containing only 13 ventilatory units and 23 airway segments. Typical reconstructions of the airway branching pattern off of the main bronchus contained 40–80 ventilatory units and 80–120 airway segments.

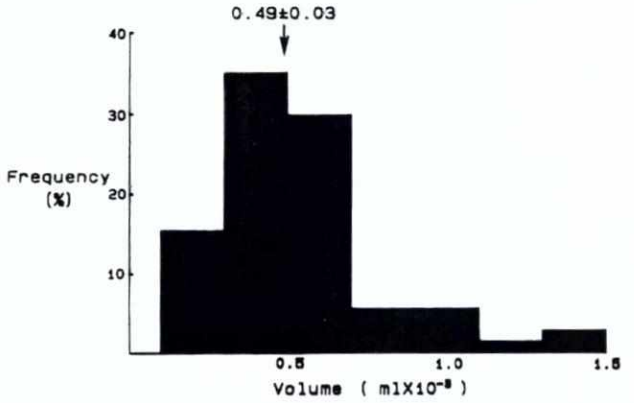


**FIGURE 6 Ventilatory unit size distribution of the rat.** The airspace volume of each ventilatory unit distal to a single airway branch off of the main stem bronchus was determined using serial sections, such as illustrated in Figure 5. This figure gives a histogram of the volume distribution of the 43 ventilatory units distal to the main stem bronchus. The histogram demonstrates a typical 10-fold variation in ventilatory unit size. The ventilatory units ventilated by these airways accounted for approximately 2% of the total lung volume alveolar volume.

of ventilation. It might be concluded from the casting studies, for instance, that differences in the degree of filling or in the compliance of different units resulted in the large variations in unit volume.

We have examined the size distribution of ventilatory units within the lungs by carrying out serial section analysis on in situ perfusion-fixed lungs at levels of lung inflation comparable to normal ventilation (Mercer and Crapo, 1989; Mercer et al., 1991). The branching patterns of airways distal to main stem bronchi of the left lungs and the outer boundaries of the ventilatory units ventilated by these airways in the lungs of rats were examined by serial-section analysis techniques. Figure 5 shows an example reconstruction from a relatively small airways off of the main stem bronchus. A reconstruction of the airways is given in the upper right of the figure and a reconstruction of the outer boundaries is shown in the lower half of the figure. From these serial sections it is possible to determine the gas volume of each ventilator unit as well as the branching pattern of alveolar ducts and alveolar sacs (terminal alveolar ducts) and the dead space/branching pattern of proximal airways.

Histograms of the volume of the ventilatory units connected to the airways in these serial section analyses have been used to determine the variation in gas-exchange unit volume between ventilatory units at functional residual capacity. An example of the histogram from one such reconstruction containing 43 ventilatory units of the rat is shown in Figure 6. The results demonstrate that ventilatory units have a considerable variation in size within local clusters of units ventilated by common airways. Indeed, it is typical to find a 15-fold difference in the size of ventilatory units distal to a single bronchus. In addition, these studies demonstrate that the size of individual alveoli within the large units is comparable to the alveolar size within the small units, and the alveolar epithelial surface to volume ratio is approximately the same for large and small ventilatory units (Mercer et al., 1991). These results would appear to exclude the potential for compliance effects causing the difference in size.

One of the major influences of variation in airway dead space and ventilatory unit size will be to vary the fraction of fresh inspired air received by each unit ($V_A$). The distribution of the ratio of ventilatory unit ventilation to ventilatory unit volume ($V_A/V$) is given in Figure 7. The results demonstrate a significant variation in the fraction of fresh inspired gas received by different ventilatory units. When comparable calculations are used to determine the variation in dose due to an inhaled, reactive, gaseous pollutant (e.g., ozone), these differences in ventilation are a significant factor in determining the variation in dose to the different ventilatory units. Approximately 5% of the ventilatory units are located on low dead space paths and have a larger than average ventilation (Mercer and Crapo, 1988b). These units have been predicted to receive a threefold or greater relative exposure to an inhaled gas due to this local variation (Mercer and Crapo, 1988b; Mercer et al., 1991). Because a comparable variation in the volume of human acini has been demonstrated by Haefeli-Bleuer and Weibel (1988), similar variations in ventilation and airborne pollutant dosimetry would also be expected. The results suggest that variation in the volume of ventilatory units is important in determining the distribution of inspired

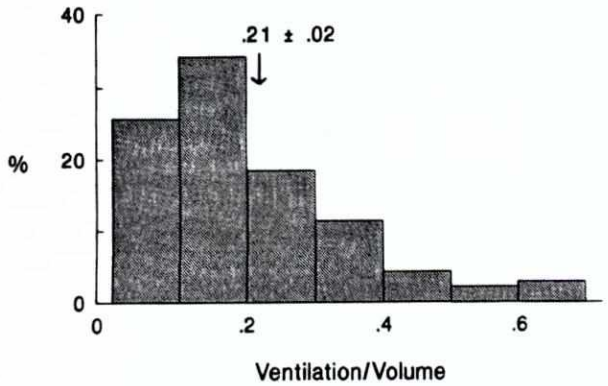


**FIGURE 7 Distribution of the ratio of inspired gas ventilating each ventilatory unit to the ventilatory unit volume.** This figure gives the histogram for the ratio of ventilatory unit ventilation to ventilatory unit volume determined from ventilation of each ventilatory unit supplied by the airways analyzed in Figure 6. The histogram demonstrates the significant variation in specific ventilation of the ventilatory units due to variations in airway dead space and ventilatory unit size. For instance, approximately 10% of the ventilatory units have a specific ventilation that is twice the mean value of 0.21, while 25% of the ventilatory units have a specific ventilation that is half the mean.

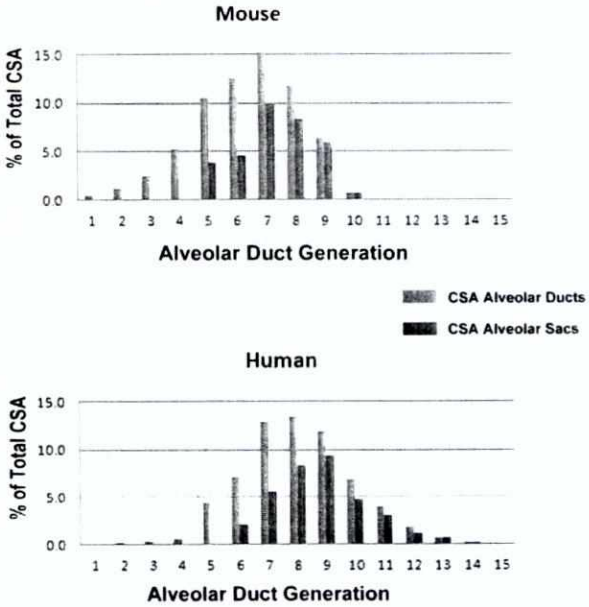


**FIGURE 8 Comparison of the branching pattern of alveolar ducts and alveolar sacs (terminal alveolar ducts) in the ventilator units of mice versus human lungs.** Figure gives plots of how the cross-sectional area of the alveolar ducts (with connected alveoli) and alveolar sacs (terminal alveolar ducts) change with generation number with the first generation beginning at the bronchiole to alveolar duct junction in the ventilator units of mouse and human lungs. The principal difference between the alveolar duct/alveolar sac branching pattern between the much smaller mouse lung and larger human lung appears to be the later occurrence of terminating alveolar sacs and a great number of subsequent generations in the larger human lung.

gas and may be particularly important in understanding the magnitude and heterogeneity of damage caused by inhalation of toxic substances. Models predicting the injury pattern due to these local variations in branching pattern and ventilatory unit size have predicted that there should be such a heterogeneity in damage (Mercer et al., 1991; Overton et al., 1996). Conformation of this pattern of injury with differences in local branching pattern and ventilator unit size has been demonstrated in the case of ozone inhalation injury (Pinkerton et al., 1992).

The serial section analysis of ventilator unit structure can also be used to investigate how the alveolar duct branching pattern varies across species. Figure 8 give example plots of how the cross-sectional area of the alveolar ducts (with connected alveoli) and alveolar sections (terminal alveolar ducts) changes with alveolar duct generation in the ventilator units of mouse and human lungs. As indicated by the lack of terminal alveolar sacs in generations 1 through 4, the first generations do not contain terminating alveolar ducts (alveolar sacs) but instead are associated with rapid dissemination of gas to more distal gas exchange regions. Across species, approximately 65 percent of the volume is present in the alveolar ducts and associated alveoli, which provide communications with more distal gas exchange regions, and 35 percent of the volume in a ventilator unit is contained in the alveolar sacs. A general bell-shaped pattern for the distribution of gas volume in the ventilatory is evident in both the mouse and human lungs. The principal difference between the alveolar duct/alveolar sac branching pattern between smaller and larger mammalian lungs appears to be the delay in occurrence of terminating alveolar sacs and a great number of subsequent generations. Data for these graphs of mouse, and human, ventilator unit branching patterns as well as those for rat and baboon are given in Table 2.

## 6. VASCULAR PERFUSION OF THE ACINUS

Not only is ventilation critical in determining dose–response relationships within the gas-exchange region of the lung but ventilation–perfusion relationships are also important, particularly for systemic delivery of inhaled gases. Of particular importance is the role variations in pulmonary capillary transit time have in determining the degree of oxygen and carbon dioxide exchange as this determines the time that transiting red blood cells have to equilibrate with the oxygen partial pressure in the lungs and to release carbon dioxide. Previous investigators have used analysis of single sections to estimate pulmonary capillary length (Staub and Schultz, 1968; Sobin et al., 1980). For instance, Sobin et al. (1980) used vascular tracers that subdivide each planar section into arteriole, venous, and capillary perfusion regions. By appropriate morphometric analysis, these investigators were able to estimate the

**TABLE 2** Species Comparison of Alveolar Duct and Alveolar Sac Branching Structure[a]

| Species | Generation | 1 | 2 | 3 | 4 | 5 | 6 | 7 | 8 | 9 | 10 | 11 | 12 | 13 | 14 | 15 |
|---|---|---|---|---|---|---|---|---|---|---|---|---|---|---|---|---|
| **Mouse Cd-1** | | | | | | | | | | | | | | | | |
| | Alveolar duct | 0.4 | 1.2 | 2.4 | 5.3 | 10.6 | 12.5 | 15.2 | 11.8 | 6.5 | 0.7 | | | | | |
| | Alveolar sac | 0.0 | 0.0 | 0.0 | 0.0 | 3.8 | 4.6 | 9.9 | 8.4 | 6.0 | 0.7 | | | | | |
| **Rat SD** | | | | | | | | | | | | | | | | |
| | Alveolar duct | 0.4 | 1.0 | 2.2 | 5.2 | 8.8 | 15.3 | 11.9 | 6.6 | 6.4 | 4.7 | 3.3 | 1.4 | | | |
| | Alveolar sac | 0.0 | 0.0 | 0.0 | 0.7 | 1.9 | 7.9 | 9.3 | 2.1 | 4.2 | 3.0 | 2.2 | 1.5 | | | |
| **Baboon** | | | | | | | | | | | | | | | | |
| | Alveolar duct | 0.1 | 0.1 | 0.3 | 0.5 | 4.2 | 8.5 | 12.8 | 14.6 | 11.5 | 6.7 | 4.0 | 1.6 | 0.7 | 0.1 | |
| | Alveolar sac | 0.0 | 0.0 | 0.0 | 0.0 | 0.0 | 2.0 | 5.7 | 8.6 | 8.0 | 4.7 | 3.4 | 1.1 | 0.5 | 0.1 | |
| **Human** | | | | | | | | | | | | | | | | |
| | Alveolar duct | 0.1 | 0.2 | 0.3 | 0.6 | 4.3 | 7.1 | 12.9 | 13.4 | 12.0 | 6.8 | 3.9 | 1.8 | 0.7 | 0.3 | 0.1 |
| | Alveolar sac | 0.0 | 0.0 | 0.0 | 0.0 | 0.1 | 2.1 | 5.6 | 8.4 | 9.5 | 4.7 | 3.2 | 1.2 | 0.7 | 0.2 | 0.1 |

[a]*Table 2 gives the volume of alveolar air in alveolar ducts (including surrounding alveoli) and in alveolar sacs (terminal alveolar ducts with surrounding alveoli) versus generation from the bronchiole–alveolar duct junction expressed as a percentage of total ventilatory unit gas volume.*

**TABLE 3 Pulmonary Capillary Length**

| Species | Capillary Length (μm) | References |
|---|---|---|
| Dog | 600–800 | Staub and Schultz (1968) |
| Cat | 556 ± 286 | Sobin et al. (1980) |
| Cat | 600–800 | Staub and Schultz (1968) |
| Rabbit | 550–650 | Staub and Schultz (1968) |
| Rat | 205 ± 8 | Mercer and Crapo (1987b) |

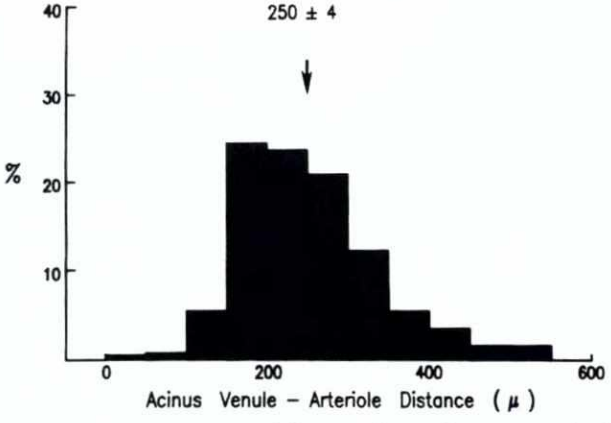


**FIGURE 9 The distribution of distances from pulmonary venules to the nearest pulmonary arteriole for blood vessels perfusing an acinus of the rat lung.**

average capillary length. The results obtained for a number of species are given in Table 3.

In addition to determining the average pulmonary capillary length, it is important to determine how the pulmonary capillary length varies within the acinus. Histograms of the acinar venule–arteriole distance, such as that given for the rat in Figure 9, suggests a significant variation in pulmonary capillary length. Based on the distances from venule to nearest arteriole and the assumption that red blood cell transit time is proportional to the square of length, a 25-fold variation in transit time could be expected in the acinus. Given the high blood flow rates present during exercise, the variation in transit time indicates that there is insufficient time for equilibration of a significant fraction of red blood cells during passage through the ventilatory unit.

## 7. SIZE LIMITATIONS IN GAS EXCHANGE

Given the quantitative descriptions of acinar structure and variations in acinar size, it is obviously of interest to consider the implications in terms of gas-exchange capacity. Illustrated in Figure 10 is a spherical model for gas

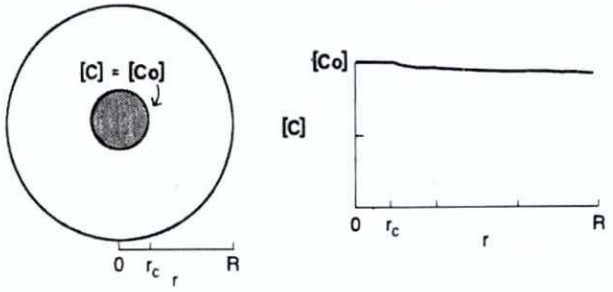


**FIGURE 10 Model for determination of gas concentration in ventilatory units.** This figure illustrates the results of a spherical model for the determination of the concentration gradients in the ventilatory unit. On the left side, the central core of the sphere is illustrated. The central core is assumed to be maintained at a constant concentration by ventilation with diffusion occurring from $r_c$, to the outer boundary at R. In both the convective and diffuse regions, it is assumed that the uptake of oxygen is occurring according to a first-order reaction (K). On the right side, the concentration profile is given for the human lung under resting conditions (K = 0.8%/s).

exchange in the ventilatory unit based on a central region maintained at a constant concentration by ventilation and an outer region where diffusion occurs. For both regions, the uptake of oxygen is proportional to the concentration.

Aside from the details of solving the equations describing this model (Appendix A), the salient features reside in three species-dependent parameters: (1) the oxygen uptake coefficient (K), (2) the size of the ventilatory unit (R), and (3) the fraction of the ventilatory unit maintained at a constant concentration core ($r_c$) by ventilation. The reaction or uptake coefficient K, which is the instantaneous rate of change in oxygen concentration, can be determined from measurements of oxygen uptake at rest and exercise (Lechner, 1978). The size of the ventilatory unit (R) is obtained from serial section reconstructions of lung preserved by vascular perfusion of fixative at functional residual volume. The size of the constant concentration region, $r_c$, is determined from the ratio of alveolar ventilation to ventilatory unit volume. The values used in the determination of oxygen uptake for rat and human lungs at rest and during exercise are given in Table 4, which also gives whole lung oxygen uptake ($VO_2$), dead space volume ($V_D$), parenchymal gas volume ($V_P$), and functional residual capacity (FRC), as well as the relevant model parameters.

Because the rate of oxygen uptake is low at rest, there is no significant gradient in oxygen concentration for small or large species, even though the constant concentration region is quite small, as illustrated in Figure 11. Of more interest is the absence of a significant concentration gradient under model conditions corresponding to exercise. This is predominately due to the dramatic increase in tidal volume, which approaches vital capacity at high levels of exercise (Murray, 1986). These results indicate that diffusional limitations in the transport of oxygen do not occur in

**TABLE 4 Respiratory Parameters in Gas Exchange**

| Species | Condition | $VO_2$ (ml/min) | $V_D$ (ml) | $V_p$ (ml) | FRC (ml) | K %/s | $r_c$ (mm) | R (mm) | % Efficiency |
|---|---|---|---|---|---|---|---|---|---|
| Rat[a] | Rest | 4.7 | 0.8 | 1.9 | 3.9 | 7 | 0.49 | 0.8 | 99 |
| | Exercise | 24.5 | 0.8 | 5.7 | 3.9 | 29 | 0.81 | 0.9 | 97 |
| Human | Rest | 250 | 190 | 600 | 2200 | 0.8 | 3.3 | 6.0 | 99 |
| | Exercise | 4000 | 190 | 2400 | 2200 | 9.3 | 5.7 | 6.6 | 95 |

[a]*Data from various sources: Mercer and Crapo (1988b), Lechner (1978), and Stahl (1967).*

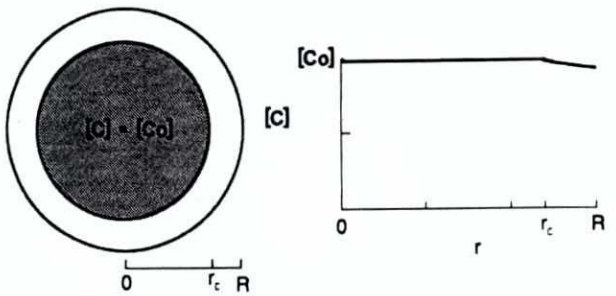


**FIGURE 11 Concentration gradients during high rates of uptake.** This figure demonstrates the conditions present during exercise where tidal volume exceeds functional residual capacity ($r_c = 0.8R$) and the uptake of oxygen is high (K = 14%/s). Under these conditions, no significant concentration gradients are predicted because of the high alveolar ventilation.

larger lungs. On the other hand, the preceding predicted variations in red blood cell transit times at high rates of exercise would appear to limit equilibration of red blood cells within the acinus and suggests that inhomogeneity in perfusion may limit maximal oxygen uptake. This influence on the inhomogeneity of perfusion may be a factor in the increased dispersion of perfusion and evidence that red blood cells failed to equilibrate on exit from the capillaries with exercise at simulated altitude (Gale et al., 1985; Wagner et al., 1986).

Weibel (1983), in a comparison of morphometric estimates of maximal oxygen uptake with physiologic determinations, concluded that there were significant diffusional limitations in larger species. This was based on modeling of diffusional uptake of oxygen in a thick slab in the absence of convective transport (DuBois and Rogers, 1968). Under resting conditions, convective transport within the acinus is only a minor component of oxygen transport, as illustrated by the size of the convective region in Figure 11. However, at moderate to high levels of exercise, as illustrated by the large increase in convective region in Figure 11, alveolar ventilation provided by increases in respiratory frequency and tidal volume is a significant contributor to convective transport in the acinus and cannot be neglected in an analysis of oxygen transport.

## 8. APPENDIX A

To determine the extent to which species variations in acinar size and intralung variations in acinar size influence gas exchange, a number of simplifying assumptions concerning the structure of the ventilatory unit must be made. The first of these will be to consider the ventilatory unit as a sphere that has a central core maintained at a constant concentration $C_o$ by ventilation. This assumption obviously differs from the traditional models, which assume a linear pattern of alveolar ducts that branch in a dichotomous pattern. However, as we have previously demonstrated, the branching pattern of the alveolar ducts is equivalent to a three-dimensional lattice or open framework.

Thus, we will consider a spherical model for determination of the concentration gradients in the ventilatory unit, as illustrated in Figure 11. This model consists of a central core that is maintained at a constant concentration by ventilation with diffusion occurring from rc to the outer boundary at R. In both the convective and diffusive regions, it will be assumed that the uptake of oxygen is linearly proportional to the oxygen concentration according to a first-order reaction coefficient k. Under these assumptions the differential equation for transport in the diffusion region is given by Eqn (1). The solution to this equation (Hershey, 1974) is given in Eqn (4), where the constants a and $a_2$ are chosen to solve the corresponding boundary conditions given in Eqns (2) and (3).

$$\frac{D}{r^2}\frac{\partial}{\partial r}\left[r^2\frac{\partial C}{\partial r}\right] - KC = 0 \tag{1}$$

$$C = C_o \text{ at } r = r_c \tag{2}$$

$$\frac{\partial C}{\partial r} = 0 \text{ at } r = R \tag{3}$$

$$C = \frac{C_o}{r}\left(a_1 \cosh\sqrt{\frac{Kr^2}{D}} + a_2 \sinh\sqrt{\frac{Kr^2}{D}}\right) \tag{4}$$

## DISCLAIMER

The findings and conclusions in this report are those of the authors and do not necessarily represent the views of the National Institute for Occupational Safety and Health.

## ACKNOWLEDGMENTS

This work was supported by US EPA Cooperative Agreement CR813113. Although the research described in this article has been funded by the US EPA, it has not been subjected to the Agency's required policy review and therefore does not necessarily reflect the views of the Agency and no official endorsement should be inferred.

## REFERENCES

Boyden, E.A., 1971. The structure of the pulmonary acinus in a child of six years and eight months. Am. J. Anat. 132 (3), 275–299.

Crapo, J.D., Barry, B.E., Change, L., Mercer, R.R., 1984. Alterations in lung structure caused by inhalation of oxidants. J. Toxicol. Environ. Health 13, 301–321.

DuBois, A.B., Rogers, R.M., 1968. Respiratory factors determining the tissue concentrations of inhaled toxic substances. Respir. Physiol. 5, 34–52.

Fouke, J.M., Delemos, R.A., McFadden Jr., E.R., 1988. Airway response to ultra short-term exposure to ozone. Am. Rev. Respir. Dis. 137, 326–330.

Gale, G.E., Torre-Bueno, J.R., Moon, R.E., Saltzman, H.A., Wagner, P.D., 1985. Ventilation-perfusion inequality in normal humans during exercise at sea level and simulated altitude. J. Appl. Physiol. 58, 978–988.

Gil, J., Bachofen, H., Gehr, P., Weibel, E.R., 1979. Alveolar volume-surface area relation in air- and saline-filled lungs fixed by vascular perfusion. J. Appl. Physiol. 47, 990–1001.

Gundersen, H.J.G., Jensen, E.B., 1987. The efficiency of systematic sampling in stereology and its prediction. J. Microsc. 147, 229–263.

Hansen, J.E., Ampaya, E.P., 1975. Human air space shapes, sizes, areas, and volumes. J. Appl. Physiol. 38, 990–995.

Hansen, J.E., Ampaya, E.P., Bryant, G.H., Navin, J.J., 1975. Branching pattern of airways and air spaces of a single human terminal bronchiole. J. Appl. Physiol. 38 (6), 983–989.

Haefeli-Bleuer, B., Weibel, E.R., 1988. Morphometry of the human pulmonary acinus. Anat. Rec. 220, 401–414.

Hershey, D., 1974. Transport Analysis. Plenum Publishing Corp, New York, N.Y.

Horsfield, K., Cumming, G., 1968. Morphology of the bronchial tree in man. J. Appl. Physiol. 24 (3), 373–383.

Kliment, V., 1973. Similarity and dimensional analysis, evaluation of aerosol deposition in the lungs of laboratory animals and man. Folia Morphol. (Praha) 21 (1), 59–64.

Lechner, A.J., 1978. The scaling of maximal oxygen consumption and pulmonary dimensions in small mammals. Respir. Physiol. 34, 29–44.

Leith, D.E., 1976. Comparative mammalian respiratory mechanics. Physiologist 19 (4), 485–510.

Macklin, C.C., 1929. The musculature of the bronchi and lungs. Physiol. Rev. 9 (1), 1–60.

Mercer, R.R., Crapo, J.D., 1987a. Determination of the pulmonary capillary length within the acinus of the rat. Fed. Proc. 46, 520.

Mercer, R.R., Crapo, J.D., 1987b. Three-dimensional reconstruction of the acinus of the rat. J. Appl. Physiol. 63, 785–794.

Mercer, R.R., Laco, J.M., Crapo, J.D., 1987. Three-dimensional reconstruction of alveoli in the rat lung for determination of pressure-volume relationships. J. Appl. Physiol. 62, 1480–1487.

Mercer, R.R., Crapo, J.D., 1988a. Structure of the gas exchange region of the lungs determined by three-dimensional reconstruction. In: Toxicology of the Lung. Raven Press, New York, pp. 43–70.

Mercer, R.R., Crapo, J.D., 1988b. Comparison of gas exchange structure across species. Am. Rev. Respir. Dis. 137, 409.

Mercer, R.R., Crapo, J.D., 1989. Anatomical Modeling of Microdosimetry of Inhaled Particles and Gases in the Lung. Extrapolation of Dosimetric Relationships for Inhaled Particles and Gases. Academic Press, New York, pp. 69–78.

Mercer, R.R., Randell, S.H., Young, S.L., 1990a. Measurement of boundaries using a digitizer tablet. J. Microsc. 160, 97–105.

Mercer, R.R., McCauley, G.M., Anjilvel, S., 1990b. Approximation of surfaces in quantitative 3-D reconstructions. IEEE Trans. BME 37, 1136–1146.

Mercer, R.R., Anjilvel, S., Miller, F.J., Crapo, J.D., 1991. Inhomogeneity of ventilatory unit volume and its effects on reactive gas uptake. J. Appl. Physiol. 70, 2193–2205.

Mercer, R.R., Russell, M.L., Crapo, J.D., 1994. Alveolar septal structure in different species. J. Appl. Physiol. 77, 1060–1066.

Mercer, R.R., Scabilloni, J.F., Hubbs, A.F., Battelli, L.A., McKinney, W., Friend, S., Wolfarth, M.G., Andrew, M., Castanova, V., Porter, D.W., 2013. Distribution and fibrotic response following inhalation exposure to multi-walled carbon nanotubes. Part Fibre Toxicol. 10, 13.

McKinney, W., Jackson, M., Sager, T.M., Reynolds, J.S., Chen, B.T., Afshari, A., Krajnak, K., Waugh, S., Johnson, C., Mercer, R.R., Frazer, D.G., Thomas, T.A., Castranova, V., 2012. Pulmonary and cardiovascular responses of rats after inhalation of a commercial antimicrobial spray containing titanium dioxide nanoparticles. Inhal. Toxicol. 24, 447–457.

Miller, F.J., Overton, J.H., Myers, E.T., Graham, J.A., 1982. Pulmonary Dosimetry of Nitrogen Dioxide in Animals and Man. Elsevier Scientific Publishing Company, Amsterdam, The Netherlands, pp. 377–386.

Murray, J.F., 1986. The Normal Lung. W.B. Saunders Co., Philadelphia.

Nadel, J.A., Colebatch, H.J.H., Olsen, C.R., 1964. Location and mechanism of airway constriction after barium sulfate microembolism. J. Appl. Physiol. 19 (3), 387–394.

Overton, J.H., Barnett, A.E., Graham, R.C., 1989. Significances of the variability of tracheobronchial airway paths and their air flow rates to dosimetry model predictions of the absorption of gases. In: Extrapolation of Dosimetric Relationships for Inhaled Particles and Gases. Academic Press, New York, pp. 273–291.

Overton, J.H., Graham, R.C., Menache, M.G., Mercer, R.R., Miller, F.J., 1996. Influence of tracheobronchial region expansion and volume on reactive gas uptake and interspecies dose extrapolations. Inhal. Toxicol. 8, 723–745.

Parker, H., Horsfield, K., Cumming, G., 1971. Morphology of distal airways in the human lung. J. Appl. Physiol. 31, 386–391.

Pinkerton, K.E., Plopper, C.G., Mercer, R.R., Roggli, V.L., Patra, A.L., Brody, A.R., Crapo, J.D., 1986. Airway branching patterns influence asbestos fiber location and the extent of tissue injury in the pulmonary parenchyma. Lab. Invest. 55, 688–695.

Pinkerton, K.E., Mercer, R.R., Plopper, C.G., Crapo, J.D., 1992. Distribution of injury and microdosimetry of ozone in the ventilatory unit of the rat. J. Appl. Physiol. 73, 817–824.

Porter, D.W., Hubbs, A.F., Chen, T.H.B., McKinney, W., Mercer, R.R., Wolfarth, M.G., Battelli, L., Wu, N., Sriran, K., Leonard, S., Andrew, M.E., Willard, P., Tsuruoka, T., Endo, M., Tsukada, T., Munekane, F., Frazer, D.G., Castranova, V., 2012. Acute pulmonary dose-responses to inhaled multi-walled carbon nanotubes. Nanotoxicology. Epub.

Pump, K.K., 1964. The morphology of the finer branches of the bronchial tree of the human lung. Dis. Chest. 46, 379–398.

Randell, S.H., Mercer, R.R., Young, S.Y., 1989. Postnatal growth of pulmonary acini and alveoli in normal and oxygen-exposed rats studied by serial section reconstructions. Am. J. Anat. 186, 55–68.

Rodriguez, M., Bur, S., Favre, A., Weibel, E.R., 1987. Pulmonary acinus: geometry and morphometry of the peripheral airway system in rat and rabbit. Am. J. Anat. 180, 143–155.

Ross, B.B., 1957. Influence of bronchial tree structure on ventilation in the dog's lung as inferred from measurements of a plastic cast. J. Appl. Physiol. 10 (1), 1–14.

Scabilloni, J.F., Wang, L., Antonini, J.M., Roberts, J.R., Castranova, V., Mercer, R.R., 2005. Matrix metalloproteinase induction in fibrosis and fibrotic nodule formation due to silica inhalation. Am. J. Physiol. Lung Cell Mol. Physiol. 288 (4), L709–L717.

Schreider, J.P., Raabe, O.G., 1981. Structure of the human respiratory acinus. Am. J. Anat. 162, 221–232.

Schroter, R.C., 1980. Quantitative comparisons of mammalian lung pressure volume curves. Respir. Physiol. 42, 101–107.

Sobin, S.S., Fung, Y.C., Lindal, R.G., Tremer, H.M., Clark, L., 1980. Topology of pulmonary arterioles, capillaries, and venules in the cat. Microvasc. Res. 19, 217–233.

Stahl, W.R., 1967. Scaling of respiratory variables in mammals. J. Appl. Physiol. 22 (3), 453–460.

Staub, N.C., Schultz, E.L., 1968. Pulmonary capillary length in dog, cat and rabbit. Respir. Physiol. 5, 371–378.

Storey, W.F., Staub, N.C., 1962. Ventilation of terminal air units. J. Appl. Physiol. 17, 391–397.

Wagner, P.D., Gale, G.E., Moon, R.E., Torre-Dueno, J.R., Stolp, B.W., Saltzman, H.A., 1986. Pulmonary gas exchange in humans exercising at sea level and simulated altitude. J. Appl. Physiol. 61, 260–270.

Weibel, E.R., 1963. Morphometry of the Human Lung. Springer-Verlag, Berlin, and Academic Press, New York.

Weibel, E.R., 1983. Is the lung built reasonably? Am. Rev. Respir. Dis. 128, 752–760.

Yeh, H.C., Schum, G.M., Duggan, M.T., 1979. Anatomic models of the tracheobronchial and pulmonary regions of the rat. Anat. Rec. 195, 483–492.

# Comparative Biology of the Normal Lung

*Second Edition*

93 - 104 2015

*Edited by*

**Richard A. Parent, PhD, DABT, FATS, RAC, ERT**
Consultox Ltd, Damariscotta, Maine

Architecture of the gas exchange region of the Lungs Mercer RR and Crapo JD

*Section editors*

*Section I*

**Kent E. Pinkerton, PhD**
Professor, Center for Health and the Environment, University of California, Davis

**Laura S. Van Winkle, PhD**
Adjunct Professor, Center for Health and the Environment, University of California, Davis

**Charles G. Plopper, PhD**
Professor Emeritus, California Primate Research Center, University of California, Davis;
Professor Emeritus, Anatomy, Physiology and Cell Biology, University of California, Davis

*Section II*

**Daniel L. Costa, MS, ScD**
National Program Director for Air, Climate & Energy, Office of Research and Development, USEPA, North Carolina;
Adjunct Professor, Environmental Science & Engineering, UNC Gillings School of Global Public Health, Chapel Hill, North Carolina

**Jeffrey S. Tepper, PhD, DABT**
Consultant and Principal, Tepper Nonclinical Consulting, San Carlos, California

*Section III*

**Debra L. Laskin, PhD**
Distinguished Professor and Chair, Department of Pharmacology and Toxicology, Ernest Mario School of Pharmacy Rutgers University, Piscataway, New Jersey

**Andrew J. Gow, PhD**
Associate Professor, Department of Pharmacology and Toxicology, Ernest Mario School of Pharmacy, Rutgers University, Piscataway, New Jersey

*Section IV*

**Richard B. Schlesinger, PhD**
Associate Dean and Professor, Dyson College of Arts and Sciences, Pace University, New York

**Gary R. Burleson, PhD**
President and CEO, Burleson Research Technologies, Inc. (BRT), Morrisville, North Carolina

ELSEVIER

AMSTERDAM • BOSTON • HEIDELBERG • LONDON • NEW YORK • OXFORD • PARIS
SAN DIEGO • SAN FRANCISCO • SINGAPORE • SYDNEY • TOKYO

Academic Press is an imprint of Elsevier